Journal of Engineering Mechanics and Machinery (2026)
Clausius Scientific Press, Canada

DOI: 10.23977/jemm.2026.110201
ISSN 2371-9133 Vol. 11 Num. 2

Research on Calibration Method of Novel Rotating Laser Profilometer

Yanyu Ding[1,2], Zhenhao Zhang[1,2,*], Dongyang Feng[1,2], Xiaojun Zhao[1,2]

[1]Tianjin Key Laboratory of Integrated Design and On-line Monitoring for Light Industry & Food Machinery and Equipment, Tianjin University of Science and Technology, Tianjin, 300457, China
[2]College of Mechanical Engineering, Tianjin University of Science and Technology, Tianjin, 300457, China
**Corresponding author: 18503579665@163.com*

Keywords: Line laser scanning; Light plane calibration; Multi-plane spatial calibration target; Error compensation; 3D Measurement

Abstract: To address the issues of multi-pose movement errors, uneven distribution of sampling points, and insufficient fitting accuracy associated with planar targets in rotary line-structured laser 3D scanning, this paper proposes an optimized light plane calibration method and target structure. Firstly, by comparing the calibration principles of planar targets, trapezoidal spatial targets, and spatial multi-planar calibration targets, a Spatial Multi-planar Calibration Target is developed to achieve single-frame synchronized acquisition at multiple depths. The covariance matrix is optimized through full-field point array constraints to enhance the accuracy of light plane fitting. Secondly, a hierarchical calibration-based installation error compensation method is established, utilizing the PnP algorithm to solve the pose relationship between sub-panels and the baseplate, thereby eliminating height and tilt deviations caused by machining and assembly. MATLAB simulation results demonstrate that the spatial multi-planar structure exhibits superior noise suppression, with a 20% improvement in the consistency of normal vector estimation. Experimental tests using standard gauge blocks and ceramic spheres show that the Mean Absolute Error of linear measurement is less than 0.0924 mm, and the measurement uncertainty within a 300 mm range is better than 0.1 mm. These results indicate that the optimized calibration method and error compensation strategy significantly improve the system's measurement accuracy and stability, meeting the requirements of industrial 3D inspection.

1. Introduction

Light plane calibration is a critical procedure in line-structured laser three-dimensional (3D) measurement systems, as it directly determines the accuracy of point cloud reconstruction and the stability of spatial coordinate computation. The equipment employed in this study is a servo-motor-driven rotating laser profilometer[1]. As the laser emitter rotates, the orientation of the emitted light plane changes accordingly. Therefore, it is necessary to calibrate the light plane parameters at multiple discrete angular positions. Conventional light plane calibration methods typically utilize a planar calibration target. By repeatedly adjusting the pose of the target, multiple sets of laser stripe

data are acquired, and the light plane equation is subsequently fitted using a least-squares approach[2]. However, this method presents inherent structural limitations: repeated manual repositioning of the calibration target can introduce pose errors, thereby constraining the overall calibration accuracy and stability. In the context of multi-angle calibration for a rotating profilometer, such errors accumulate and amplify with increasing calibration times, making it difficult to satisfy high-precision measurement requirements, as illustrated in Figure 1.

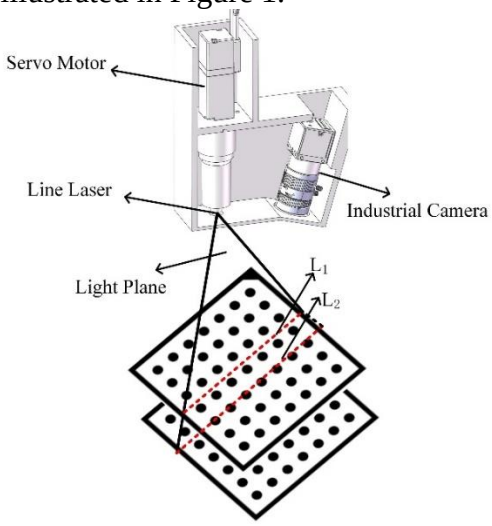

Figure 1: Light plane calibration method based on a planar target

To improve the sampling range and the uniformity of geometric constraints within a single frame, trapezoidal spatial calibration targets have been proposed to enable multi-depth acquisition in one capture. Nevertheless, the upper planes are typically concentrated near the central region, resulting in a step-like and locally distributed laser stripe point cloud, which limits the effectiveness of geometric constraints.

To address these issues, this paper proposes a spatial multi-plane calibration target. By arranging sub-planes at the four corners and the center of a base plate, synchronous multi-depth acquisition across the entire field of view can be achieved within a single frame. This configuration promotes isotropic sampling constraints and optimizes the eigenvalue distribution of the covariance matrix. To compensate for assembly errors, a hierarchical calibration error compensation method is further introduced. The pose relationship between each sub-plane and the base plate is solved using a Perspective-n-Point (PnP) algorithm, thereby eliminating height and tilt deviations. Experimental results indicate that the angular range from $30°$ to $150°$ provides reliable laser stripe data for calibration. Both simulation and physical experiments demonstrate that the proposed method improves light plane fitting accuracy and measurement stability, offering an efficient and high-precision calibration solution for line-structured laser 3D measurement systems, as illustrated in Figure 2.

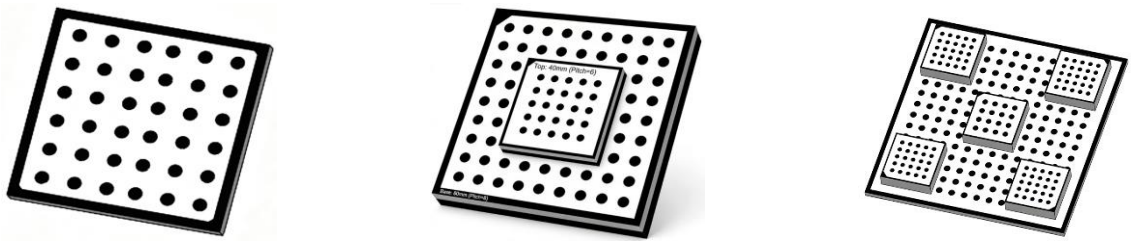

(a) (b) (c)

Figure 2: Comparison of different calibration targets

2. Improvement of the Light Plane Calibration Method and Design of a Spatial Multi-Plane Target

This chapter focuses on the light plane calibration method for a line-structured laser measurement system. First, the calibration principle and procedure based on a conventional planar target are described, and its limitations—such as errors introduced by repeated pose adjustments and restricted sampling coverage—are analyzed. On this basis, a trapezoidal planar calibration target and a spatial multi-plane calibration target are proposed. By enabling single-frame multi-depth acquisition and full-field geometric constraints, the light plane calibration method and target structure are optimized, providing theoretical support for high-precision calibration.

2.1. Principle of Light Plane Calibration Based on a Planar Target

Based on the pinhole camera imaging model, the two-dimensional laser stripe observed in the image plane is in fact the projection formed by the intersection of the spatial light plane and the camera imaging plane. Let the intrinsic camera matrix parameters be (f_x， f_y， u_0， v_0). After fitting, the laser stripe in the image coordinate system satisfies the following line equation:

$$u = av + b \tag{1}$$

According to the perspective projection relationship and the translation–scaling model, a normalized plane can be established to construct the mapping between the image pixel coordinates (u， v) and the three-dimensional coordinates (X_1， Y_1， 1) in the normalized plane:

$$\begin{aligned} u &= f_x X_1 + c_x \\ v &= f_y Y_1 + c_y \end{aligned} \tag{2}$$

By back-projecting the pixel line equation into three-dimensional space, the equation of the viewing plane passing through the camera optical center can be derived as:

$$af_x X_c - f_y Y_c + \left(ac_x + b - c_y\right) Z_c = 0 \tag{3}$$

During calibration, the origin of the world coordinate system is defined at the upper-left corner of the checkerboard, and the checkerboard plane is assumed to coincide with the plane Z_w=0 of the world coordinate system. According to rigid body transformation theory, a point P_w in the world coordinate system and its corresponding point P_c in the camera coordinate system satisfy the transformation relationship P_c=RP_w+tP_c[3]. Since the points on the calibration board satisfy Z_w=0, the general plane equation of the calibration board in the camera coordinate system can be derived from the rotation and translation components of the extrinsic matrix as:

$$A_p X_c + B_p Y_c + C_p Z_c + D_p = 0 \tag{4}$$

Here, the normal vector of the plane is determined by the third column of the rotation matrix R, and the constant term D_p is given by the dot product of the translation vector t and the plane normal vector. Finally, by combining the previously derived viewing plane equation of the laser stripe with the plane equation of the calibration board, a linear system of equations can be constructed. The unique intersection line of these two spatial planes corresponds to the true three-dimensional laser stripe line projected onto the calibration board in the camera coordinate system. Its mathematical expression is:

$$\begin{cases} af_x X_c - f_y Y_c + \left(aC_x + b - C_y\right) Z_c = 0 \\ A_p X_c + B_p Y_c + C_p Z_c + D_p = 0 \end{cases} \tag{5}$$

By varying the pose of the calibration board, typically by positioning it at two or more different heights, the above procedure is repeated to obtain multiple sets of three-dimensional laser stripe lines at different spatial locations. Using the least-squares method, all reconstructed laser stripe points are fitted to a spatial plane, ultimately yielding the equation of the light plane for the line-structured laser profilometer.

2.2. Design and Investigation of the Trapezoidal Spatial Target and the Spatial Multi-Plane Target

To overcome pose measurement errors introduced by manual repositioning of the calibration board in conventional methods, this study proposes single-frame synchronous multi-depth acquisition based on a trapezoidal spatial target and a spatial multi-plane calibration target[4]. The trapezoidal planar target consists of a base plate and an upper plate, with a known height difference h between them. In the definition of the world coordinate system, the base plate satisfies Z_w=0, while the upper plane satisfies Z_w=h. In a single captured image, the laser stripe is simultaneously projected onto both height planes. According to the derivation presented above, two spatial lines can be obtained respectively:

$$\begin{cases} L_1 : P_1(t) = P_{01} + td_1, Z_w = 0 \\ L_2 : P_2(s) = P_{02} + sd_2, Z_w = h \end{cases} \tag{6}$$

where P_{01} and $P_{02}$are points on the respective spatial lines, and t and s denote their direction vectors. Since the light plane is uniquely determined, the two spatial lines must lie on the same laser plane. All spatial points are then fitted using the least-squares method to construct the following optimization objective function[5]:

$$\min_{A,B,C,D} \sum_{i=1}^{L_1+L_2} (Ax_i + By_i + Cz_i + D)^2 \tag{7}$$

Compared with the traditional method, the trapezoidal structure enables single-frame calibration. However, the upper plane is concentrated near the central region of the calibration board, resulting in a step-like and locally distributed laser stripe point cloud. In contrast, the proposed spatial multi-plane calibration target arranges sub-plates at the four corners and the center of the base plate, allowing the laser line to span the entire field of view simultaneously. The covariance matrix of the point cloud distribution in the horizontal direction can be expressed as:

$$C = \frac{1}{N} \sum_{i=1}^{N} \left(X_i - \overline{X}\right)\left(X_i - \overline{X}\right)^T \tag{8}$$

The geometric constraints in both the horizontal length and width directions become balanced and approach isotropy, $\lambda_1 \approx \lambda_2 \gg \lambda_3$, thereby reducing the condition number. The covariance of the estimated light plane normal vector can be expressed as:

$$Cov(n) = \frac{\sigma_p^2}{N} C^{-1} \tag{9}$$

With the reduction of the condition number of matrix C, the estimation variance decreases as the

baseline length increases. By maximizing the spatial geometric baseline, the spatial multi-plane calibration target transforms local sampling into full-field point-array constraints[6].Mathematically, this design optimizes the eigenvalue distribution of the covariance matrix, evolving from a quasi-linear configuration to an isotropic distribution, thereby achieving higher-precision light plane fitting[7].

3. Performance Simulation and Error Analysis of the Spatial Multi-Plane Target

This chapter presents simulation verification and error characteristic analysis of the calibration system. MATLAB simulations are conducted to validate the noise robustness and fitting advantages of the proposed spatial multi-plane calibration target. To address practical assembly errors, a hierarchical calibration error compensation method is proposed. In addition, laser stripe angle experiments are carried out to determine the reliable calibration interval, thereby standardizing the calibration procedure and correcting systematic errors. These efforts lay the foundation for subsequent physical experiments.

3.1. MATLAB-Based Simulation of Multi-Light-Plane Fitting

To verify the geometric advantages of the proposed spatial multi-plane calibration target, an ideal calibration model is first established through numerical simulation.

A virtual pinhole camera model is constructed in MATLAB, with a focal length of 12 mm and a resolution of 1280*1024 pixels. According to the design drawings, a three-dimensional model of the standard five-point composite calibration board is established. The theoretical height difference between the base plate and each of the five sub-plates is set to h=5.0000 mm. A line-structured laser plane is simulated to scan across the field of view at different pitch angles. During feature extraction, Gaussian white noise with a standard deviation of 0.5 pixels is added to the pixel coordinates to simulate real environmental disturbances[8] . Using the reprojection model described in Chapter 2, the three-dimensional point cloud is reconstructed, and principal component analysis (PCA) is applied to fit the light plane[9]. The scanning process is illustrated in Figure 3.

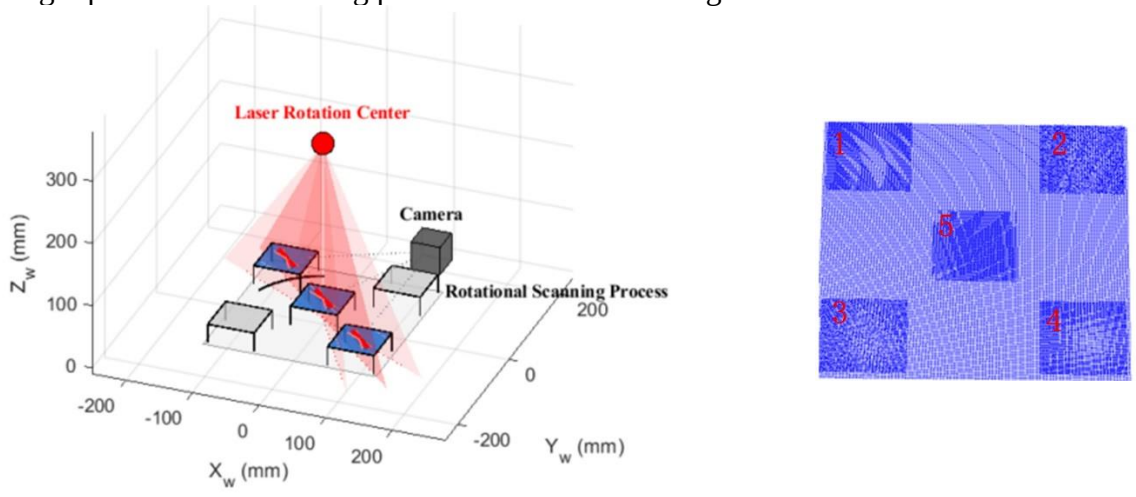

(a)Schematic diagram of the simulation setup (b)Simulated point cloud

Figure 3: Simulation experiment of the proposed calibration board

The root mean square error (RMSE) between the reconstructed point cloud and the fitted plane is calculated. Ten repeated height reconstruction experiments show that, compared with the planar target under identical conditions, the average measured heights of sub-plates 1, 4, and 5 obtained using the spatial multi-plane calibration target are all less than 5.005 mm, demonstrating significantly improved

reconstruction accuracy and stability. However, the reconstructed results for sub-plates 2 and 3 exhibit a noticeable systematic deviation of approximately 0.1 mm. This phenomenon occurs because, during rotational scanning of the laser plane, the projection angle of the laser stripe in the image coordinate system continuously changes. When the laser stripe rotates to a nearly horizontal orientation, the deformation distance in the triangulation geometry approaches zero. Consequently, geometric degeneration occurs in the system's perception of height information, preventing effective discrimination of height differences between planes in the real world. A detailed analysis is provided in Section 3.3. These results demonstrate that, under ideal geometric conditions, the proposed design enhances height measurement accuracy and noise robustness within the effective field-of-view range, as illustrated in Table 1.

Table 1: Verification of height measurement accuracy in simulation

No.	Sup-plate 1	Sup-plate 2	Sup-plate 3	Sup-plate 4	Sup-plate 5
1	4.9923	5.1127	5.0984	4.9876	5.0031
2	5.0048	5.1256	5.1079	4.9954	4.9987
3	4.9891	5.0963	5.0892	5.0023	4.9915
4	4.9976	5.1342	5.1187	4.9819	5.0064
5	5.0087	5.1078	5.0921	4.9942	4.9958
6	4.9834	5.1195	5.1046	5.0078	5.0012
7	4.9965	5.0884	5.0763	4.9897	4.9976
8	5.0021	5.1413	5.1234	4.9965	5.0043
9	4.9912	5.1037	5.0958	5.0084	4.9929
10	4.9987	5.1279	5.1105	4.9821	5.0078
Mean Absolute Error	0.0068	0.1185	0.1012	0.0089	0.0047
Standard Deviation	0.0072	0.0159	0.0138	0.0086	0.0051

3.2. Sub-Plate Pose Identification and Error Compensation Based on PnP

During the assembly of the physical prototype, the sub-plates are fixed to the base plate by adhesive bonding or screws. Due to manufacturing and assembly tolerances, the actual height often deviates from the theoretical value of 5 mm, and slight tilting may occur.

To eliminate the influence of assembly errors on light plane calibration accuracy, this paper proposes a pose identification algorithm between plates based on extrinsic parameter closed-loop derivation. At the calibration site, the camera first captures an image of the stationary composite calibration board. Using the feature point set of the base plate and those of each sub-plate, the PnP algorithm is independently applied to solve for the pose of the camera relative to the base plate world coordinate system, P_w, and the pose of the camera relative to the local coordinate system of the k-th sub-plate, P_{lk}. According to the coordinate transformation relationship, the actual transformation matrix of the k-th sub-plate relative to the base plate can be expressed as:

$$Pw = T_{lk}^{w} P_{lk} \tag{10}$$

where:

$$T_{lk}^{w} = \begin{bmatrix} R_{lk} & t_{lk} \\ 0 & 1 \end{bmatrix} \tag{11}$$

From the translation vector t_{lk} of this matrix, the precise actual installation height h_k of each sub-plate can be extracted, and the tilt deviation can be identified from the rotation component, as illustrated in Figure 4.

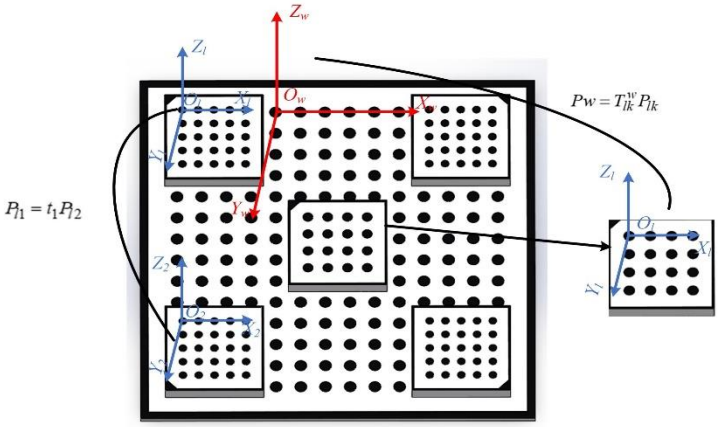

Figure 4: Hierarchical coordinate transformation

Through the above pose transformation matrix, the true installation height of each sub-plate is obtained from the translation component, and the tilt deviation is identified from the rotation component, enabling precise compensation for assembly errors. After compensation, the calibration system effectively eliminates height and angular deviations caused by manufacturing and assembly errors[10]. The reconstructed laser stripe point cloud more closely conforms to the theoretical light plane, reducing plane fitting residuals and improving the consistency and stability of light plane normal estimation. Experimental verification of the compensation accuracy improvement is presented in Chapter 4.

3.3. Operational Procedure of the Spatial Multi-Plane Target

To ensure calibration accuracy and reconstruction stability of the proposed rotating line-structured laser 3D measurement system, light plane calibration must first be performed over the full angular range (0 °,180 °). The experiment adopts a multi-light-plane calibration method[11] , with an angular interval of 1 °, resulting in a total of 181 calibrated light planes.

After calibration, the system scans a reference plane to generate its three-dimensional point cloud data. The point cloud in the camera coordinate system is then transformed into the reference plane coordinate system for analysis. The results are shown in Figure 5. When the laser stripe angle approaches 0 ° or 180 °, the corresponding reconstructed point cloud distribution becomes more disordered, characterized by increased plane thickness and more scattered points. To ensure measurement accuracy, laser stripe angles yielding a reconstructed Z-value less than 0.05 mm are considered successful calibration angles. Ultimately, the angular range (30 °, 150 °) is determined as the reliable light plane calibration interval[12].Therefore, when using the proposed calibration board for light plane calibration, the diagonal region of the board covering three sub-plates, should be arranged to maximally cover the optimal light plane range.

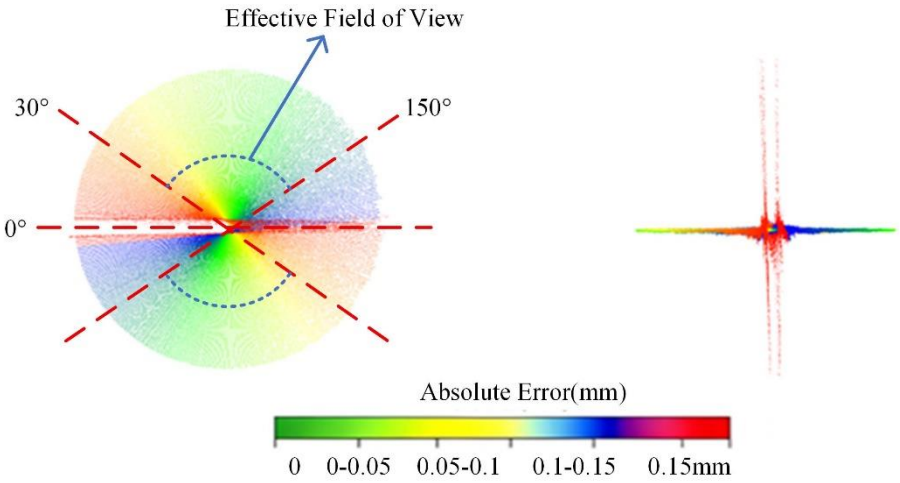

(a)Top view (b)Side view

Figure 5: Accuracy distribution in the scanning field of view

The fundamental reason for the limitation of the effective angular range lies in the variation of the laser stripe deformation distance during rotational scanning. As the laser rotates, the laser stripe in the image correspondingly rotates. Under ideal conditions, when the laser stripe forms a certain angle with the horizontal direction, as shown in Figure 6(a), planes of different heights on the measured object produce a distinct deformation distance in the image, effectively reflecting real-world height differences and enabling valid light plane calibration. However, when the laser stripe angle approaches the horizontal direction, the deformation distance correspondingly approaches zero. Once the stripe becomes completely horizontal, the deformation distance reduces to zero, as shown in Figure 6(b). At this point, the laser stripe loses sensitivity to height information and cannot distinguish height differences between planes, resulting in calibration failure at that angular position.

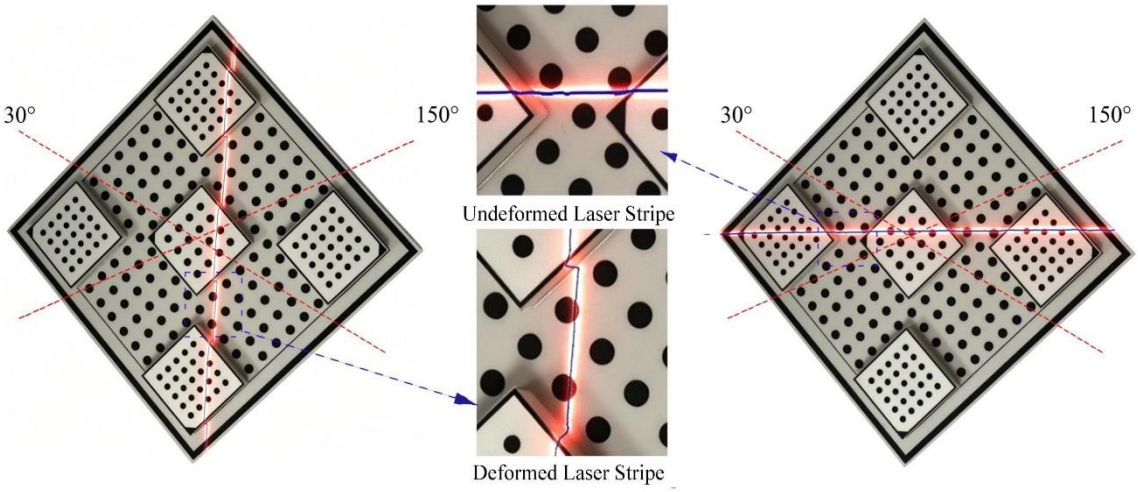

Figure 6: Distribution of laser stripe centers in different scanning regions

4. Experimental Design and Analysis

In this study, a standard gauge block and a ceramic sphere were selected as test objects. The nominal height of the standard gauge block is 5 mm±0.001 mm. The gauge block was measured ten times using a HandySCAN Black Elite 3D scanner, yielding an average measured height of 4.988

mm. The gauge block was then placed on a rotating stage, and the system drove the laser probe to perform circumferential scanning. The acquired point cloud data were first processed using a statistical filter to remove outliers. Subsequently, a plane segmentation algorithm based on Random Sample Consensus (RANSAC) was applied to extract the top surface point cloud set P_{top} and the reference plane point cloud set P_{base}[13]. The dimensional measurement focused primarily on the height of the gauge block. The measured height H_{meas} was defined as the Euclidean distance between the fitted plane of the top surface and the fitted plane of the reference surface. Ten repeated measurements were conducted, and the mean absolute error (MAE) and standard deviation were calculated, as illustrated in Table 2.

Table 2: Verification of height measurement accuracy for the standard gauge block

No.	Planar Target	Spatial Multi-Plane Target(Uncompensated)	Spatial Multi-Plane Target(Compensated)
1	5.1207	5.1426	5.03387
2	5.1184	5.1573	5.1085
3	5.1352	5.1289	5.10619
4	5.1096	5.1634	5.09726
5	5.1271	5.1357	5.11080
6	5.1413	5.1702	4.95717
7	5.1135	5.1518	5.10763
8	5.1309	5.1245	5.06235
9	5.1028	5.1689	5.07670
10	5.1246	5.1390	5.01907
Mean Absolute Error	0.1224	0.1482	0.0765
Standard Deviation	0.0118	0.0165	0.0109

To further evaluate the system's capability for freeform surface measurement, a high-precision matte ceramic sphere was selected as the test object. The ceramic sphere features an extremely low thermal expansion coefficient and excellent sphericity, making it suitable for evaluating the system's comprehensive geometric error in three-dimensional space. The nominal diameter of the standard sphere is D_{ref}=20 mm, with a sphericity error less than 0.01 mm. The HandySCAN Black Elite 3D scanner was used to measure the standard ceramic sphere ten times, yielding an average measured diameter of 20.005 mm, as illustrated in Figure 7.

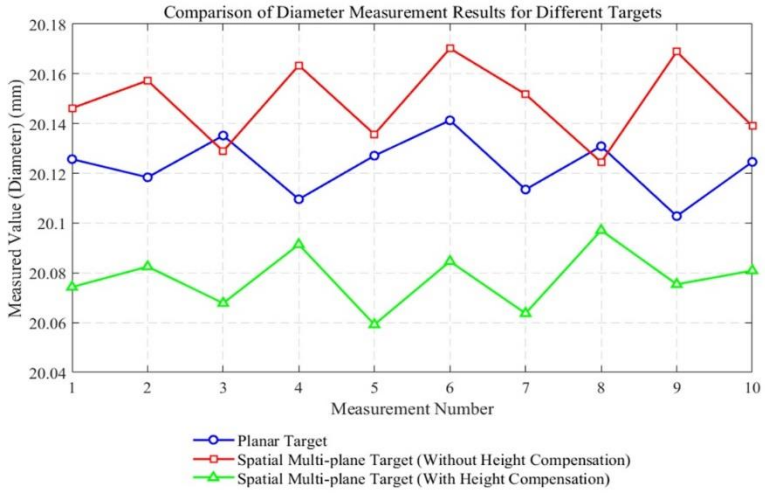

Figure 7: Direct measurement accuracy verification of the ceramic sphere

Under a constant-temperature laboratory environment, the standard gauge block and high-precision ceramic sphere were selected as experimental objects The experimental setup is shown in Figure 8. For the dimensional measurement of the standard gauge block, the system achieved a linear measurement mean absolute error better than 0.0777 mm, with repeatability of ±0.0125 mm. For the diameter measurement of the standard ceramic sphere and spherical fitting residual analysis[14], as illustrated in Figure 9. For the diameter measurement of the standard ceramic sphere and spherical fitting residual analysis[15]. The system satisfies the practical requirements of industrial inspection applications.

Figure 8: Experimental setup

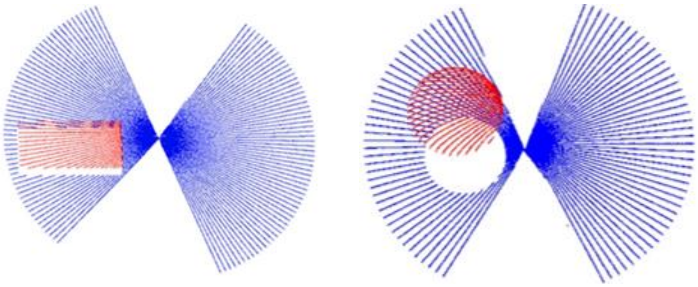

Figure 9: Scanned 3D point cloud

5. Conclusion

This study completes the optimization of the light plane calibration method and the structural design of the calibration target for a line-structured laser measurement system. A spatial multi-plane calibration target and a hierarchical installation error analysis strategy are proposed. Simulation and experimental results demonstrate that the spatial multi-plane target effectively reduces the influence of noise and significantly improves the consistency of light plane normal estimation. The proposed error compensation method eliminates assembly deviations and further enhances measurement accuracy. The optimal laser stripe angular range for calibration is determined to be 30 °–150 °, ensuring stable system operation.

Validation experiments using a standard gauge block and a ceramic sphere confirm that the system's measurement accuracy meets the requirements of industrial inspection. This research improves the calibration efficiency and measurement reliability of line-structured laser 3D scanning systems and can be extended to various structured-light 3D measurement applications.

Acknowledgement

This work was supported by the Foundation of Tianjin Key Laboratory of Integrated Design and On-line Monitoring for Light Industry & Food Machinery and Equipment (Tianjin University of Science and Technology) (No.2024LIMFE04); Tianjin Metrology Technology Project under Grant number 2024TJMT031.

References

[1] Ha V T, Do V P, Lee B R, Calibration method of a three-dimensional scanner based on a line laser projector and a camera with 1-axis rotating mechanism[J]. Optical Engineering. 2024, 63(5): 033101.
[2] Gao H, Xu G, Ma Z. A Novel Calibration Method of Line Structured Light Plane Using Spatial Geometry[J]. Sensors, 2023, 23(13): 5929.
[3] Li T, Liu C, Duan F, Fu X, Niu G., Liang C, Chen A, A light plane calibration method of line-structured light sensors based on unified extrinsic parameters estimation, Optics and Lasers in Engineering. 188 (2025) 108925.
[4] Li X, Zhang W, Song G, Calibration Method for Line-Structured Light Three-Dimensional Measurement Based on a Simple Target, Photonics. 9 (2022) 218.
[5] Zhu Z, Liu H, Zhang J, et al. Calibration method of line-structured light sensors based on a hinge-connected target with arbitrary pinch angles[J]. Applied Optics, 2023, 62(7): 1695–1703.
[6] Li C, Xu X, Ren Z, et al. Research on Calibration Method of Line-Structured Light Based on Multiple Geometric Constraints[J]. Applied Sciences, 2023, 13(10): 5998.
[7] Zhao X, Li T, Yang Z, A novel method to calibrate the rotation axis of a line-structured light 3-dimensional measurement system, Optics and Lasers in Engineering. 164 (2023) 107496.
[8] Carmignato S, Gebhardt M, Kruth J P. Uncertainty evaluation in dimensional measurements by laser triangulation[J]. CIRP Annals - Manufacturing Technology, 2020, 69(1): 485-488.
[9] Ling Y, Wang Y, Chan T O. RANSAC-Based Planar Point Cloud Segmentation Enhanced by Normal Vector and Maximum Principal Curvature Clustering[J]. ISPRS Annals of Photogrammetry, Remote Sensing and Spatial Information Sciences, 2024, 145–151.
[10] Gestel N V, Cuypers S, Bleys P, et al. Systematic error compensation for laser line scanners based on calibration artefacts[J]. Precision Engineering, 2021, 72: 538-549.
[11] Zhao J, Cheng Y, Cai G, He S, Liao L, Wu G, Yang L, Feng C, A Calibration Method for a Self-Rotating, Linear-Structured-Light Scanning, Three-Dimensional Reconstruction System Based on Plane Constraints, Sensors. 21 (2021) 8359.
[12] Zhao H, Liu X, Wang S, Diao K, Luo C. Calibration method of a three-dimensional scanner based on a line laser projector and a camera with 1-axis rotating mechanism[J]. Optical Engineering, 2024, 63(3): 033101.
[13] Guo X, Li J, Peng Y, et al. Three-Dimensional-Scanning of Pipe Inner Walls Based on Line Laser[J]. Sensors, 2024, 24(11): 3620.
[14] Li C, Fang C, Zhang X. Automated line scan profilometer based on the surface recognition method[J]. Optics and Lasers in Engineering, 2024, 182: 108464.
[15] Wang R, Li C, Li H, Wang Y, Huang Z, Rotation Scanning and Double Precision System for Three-Dimensional Geometric On-Machine Measurement, Measurement. (2025) 117581.